

On Navier slip and Reynolds transpiration numbers

PAWEŁ ZIÓŁKOWSKI, JANUSZ BADUR

*Energy Conversion Department
Institute of Fluid Flow Machinery
Polish Academy of Sciences
Fiszera 14
80-231 Gdańsk, Poland
e-mails: pawel.ziolkowski@imp.gda.pl,
jb@imp.gda.pl*

IN THIS PAPER, BASED ON THE ORIGINAL ARGUMENTATION of Reynolds and Maxwell, with consideration of previous experiences of the authors in the nano- and micro-flows area, a general form of boundary forces, that consist of contributions from the friction and the mobility components: $\mathbf{f}_{\partial V} = \mathbf{f}_r + \mathbf{f}_m$, has been extended to common effects of the bulk and surface motion. Hence, adopting Reynolds' reasoning to a porous media as a whole, we reexamine the Poiseuille–Knudsen–Reynolds equation in terms of the sum of three contributions: the bulk pressure-driven flow, and two mobility surface forces, namely the Knudsen surface slip-driven flow and the Reynolds surface thermally-driven flow. The main motivation of our work is to find the dimensionless contribution of the Navier slip number and the Reynolds thermal transpiration number in materials with high volumetric surface density.

Key words: micro- and nano-flows, slip velocity, pressure-driven flow, thermally-driven flow.

Copyright © 2018 by IPPT PAN

1. Introduction

THE BASIC GOAL OF BOTH EXPERIMENTAL AND NUMERICAL MICRO-MECHANICS is to identify a main (even fundamental) difference between the macro-scale and the micro/nano-scale. Recently, CELATA *et al.* [1], COLIN [2], KARNIADAKIS *et al.* [3] have described in the literature this difference as scaling effects. Only by careful study of the differences between macro-systems and micro/nano systems, can a basic feature of nanotechnology and its unusual possibilities and high-performance be identified. However, effects that are not important in macro-scale, become crucial phenomena when the characteristic dimensions of a system decrease. When speaking about dimensions we usually mean the hydraulic diameter of a canal which in micro-systems varies from 2 μm to 300 μm . But a more universal, and also more practical parameter, is the volumetric surface density:

“ $a_v = \text{wall surface/volume}$ ”, which in micro-systems attains $a_v = 5000 \text{ m}^2/\text{m}^3$ and in nano-systems varies between $20 < a_v < 300 \text{ km}^2/\text{m}^3$ KARNIADAKIS *et al.* [3].

In the literature, the primary and frequently stated physical postulate of nanomechanics is that a_v is a leading factor of the scaling effects for porous media, where bulk flow resistance, surface flow resistance and surface mobility forces are combined. It means that when $a_v \rightarrow \infty$ the surface properties of solid and contacting fluid becomes dominant over well-known classical properties of fluids in bulk; for instance, when $a_v > 50 \text{ km}^2/\text{m}^3$ then viscosity of a fluid can be omitted from consideration and only the surface effects give important contributions to the flow resistance.

In the literature another scaling effect parameter could be found yet. It is the slip length $l_s = \mu/\nu$, related to surface viscosity, where μ is the fluid internal viscosity. Frequently, it has been assumed that the scaling effect dominates when the slip length becomes comparable with a radius of a micro-tube; $l_s \sim d/2$ MORINI *et al.* [4]. Of course, it is obviously true but only in a particular situation when the slip resistance dominates in a micro-flow.

In the present paper we propose to replace the parameter l_s by the already averaged equations for the bulk flow resistance and the surface mobility forces. The uniqueness of l_s comes from the fact that the Navier surface viscosity ν describes only a small part of the *vis impressa* traction boundary force $\mathbf{f}_{\partial V}$. Generally, the surface force $\mathbf{f}_{\partial V}$ is composed of the friction and mobility components, $\mathbf{f}_{\partial V} = \mathbf{f}_r + \mathbf{f}_m$. The friction force can be considered as the Navier slip force $\nu \mathbf{v}_s$ which has only limited importance. In other words, adopting Reynolds’ reasoning to porous media as a whole, we reexamine the Poiseuille–Knudsen–Reynolds equation in terms of the sum of three contributions: the bulk pressure-driven flow, and two mobility surface forces, mainly: the Knudsen surface slip-driven flow and the Reynolds surface thermally-driven flow.

There are two fundamental and universal integral characteristics related to pressure derived flows of a fluid through any canal, independent of its size and length. The first one describes the mass flow rate derived by a unit drop of pressure; $c = \dot{m}/\Delta p$ [kg/sPa]. The second one is the dimensionless flow resistance measured by the so-called friction factor. It is connected with the frictional pressure loss observed for a unit mass flow rate $\dot{m} = 1 \text{ kg/s}$ during a fluid flow. The friction factor f_{SP} is defined as the dimensionless wall stress τ_w observed during flow of fluid $\dot{m} = 1 \text{ kg/s}$ and is denoted as $f_{SP} = \tau_w/(\rho u^2)_{\dot{m}=1}$. Now, the main question, which is stated in the contemporary literature, is: does the friction factor depend on the scale effect, or, mathematically speaking is f_{SP} a function of the slip length $l_s = \mu/\nu$?

An answer to this question has been developed in Sections 2 and 3, where concepts of flow resistance are divided between internal and external friction. In Section 4 the REYNOLDS discovery [5, 6] of thermal transpiration has been

considered. Unfortunately, he had his own explanation of thermal transpiration and, contrary to MAXWELL [7], his own line of reasoning. Reynolds asserts that the primary reason for thermal transpiration in the bulk motion is not the second gradient of temperature along the axis of a capillary, but the axial gradient of acceleration. When it acts close to the wall surface it can prompt the enhancement (increase) of the normal velocity slip. It is also connected with a higher value of the slip length $l_s = \mu/\nu$, but ν rather decreases due to the mobility effect.

The main motivation of our work is to find the dimensionless contribution of the Navier slip number (Na) and Reynolds thermal transpiration number (Ret) in materials with the high a_v volumetric surface density.

2. Concept of the flow resistance

The friction factor is undoubtedly one of the most important engineering parameters, especially for the design of micro-devices of MEMS (Micro-Electro-Mechanical-Systems) and NEMS (Nano-Electro-Mechanical-Systems). In order to define it we need an experimentally given drop of pressure $dp/dx = (p_{in} - p_{out})/L$, where $p_{in} - p_{out}$ is the pressure drop by flow through a distance L . Therefore, it brings only some integral information about the fluid resistance. Furthermore, a primary aim of experimental efforts to separate the effects of skin (surface) resistance and internal flow resistance does not have a rational basis [4, 8–11]. On the other hand, comprehensive experimental data is necessary for calibration and comparison with mathematical models. The objective of this section is the development of state-of-the-art of gas flow with respect to coupled effects of internal and external friction of fluid.

Let us recall that our continuum modeling of gas flow usually deals with the so-called slip regime $0.001 < Kn < 0.1$ [12]. This flow regime is correctly described by the classical MAXWELL [7] slip model. It is based on an assumption that shear viscous stresses are described correctly by a constant viscosity and the Navier dimensionless slip length is not a constant constitutive quantity, and follows linearly from the Knudsen number, $Na = Kn(2 - f)/f$, whereas, the momentum accommodation coefficient is constant: $f = \text{const}$. But if the characteristic dimension of the canal is decreased significantly, then Kn increases its value, removing the characteristic picture of gas flow into the transition regime. However, it is not a state of gas rarefaction since the pressure is standard (atmospheric) and the gas is dense.

Such a case, for instance, was considered in an experiment by MAURER *et al.* [13] with the inlet pressure p_{in} approximating atmospheric conditions, namely: 0.26–5 bar for Helium; 0.14–3.5 for Nitrogen. The authors obtained high Knudsen numbers ($0.06 < Kn < 0.8$ Helium; $0.002 < Kn < 0.59$ Nitrogen) owing to the application of a small micro canal (1.14 μm deep and 200 μm wide) covered

by an atomically flat silicon wafer. This case precisely demonstrates the scaling effect, which means that the bulk properties of the flow are less important and we can keep the viscosity of fluid as constant. The extension of the Knudsen number from the slip to the transition regime due to decrease of the diameter of the micro canal should take into account an analogical extension of the Navier–Stokes model. Therefore, this can be done by enhancement of the Maxwell slip law into a more complex description which takes into account the non-linear relation between velocity slip and the Knudsen number [14–17] the second-order boundary conditions [18, 19].

However, when the average pressure of gas decreases and attains a value identified as a vacuum (1–10 torr), then, even for normal macro tubes, the Knudsen numbers are high and indicative of a rarefaction state. But it is a case when the scaling effect is not present and can be omitted from the mathematical modeling. According to the kinetic theory of gases [20] the rarefaction state needs some change in the modeling of the stress tensor. Usually it is obtained by changing expressions on the shear stress by taking a second-order Chapman–Cowling approximation, without changing of the no-slip boundary conditions.

From the numerical modeling point of view, the most complex case can be found in the MEMS and NEMS divides, where both the rarefaction and the scaling effect are present simultaneously. This case is also challenging for experimental mechanics [2, 21–23]. It appears that there is some traditional treatment of both these effects in terms of the Knudsen number. Therefore, sometimes we have a problem with exposing separate influences of the rarefaction and the scaling effects. Thus, in the paper we describe rarefaction effects in terms of the Knudsen number, and the scaling effects in terms of other numbers, for instance, the Navier number.

2.1. Internal friction of fluid lamina

The subject of flow resistance, since the time of the appearance of Newton’s *Principia*, was perhaps studied as a composition of two kinds of friction. The first kind of friction was related to internal attrition of fluid laminas and therefore was regarded to be the internal friction of a fluid substance [24]. The laws of internal friction, proposed by NEWTON [24], and today known as “Newtonian fluid”, assume that the force of internal resistivity is proportional (linear) to the velocity gradient normal to the direction of the motion of the fluid. The coefficient of proportionality, named by Stokes, “viscosity” since it was derived from the Latin word “*viscoum*”, and denotes the property of lamina gluing [25, 26]. Yet another associated word “*viscid*” has been used for this mode of internal friction. Thus, today the word “*inviscid*” is often used to imply that a fluid is not viscous.

But the first, more primary mode of internal friction between lamina is connected with the phenomenon of stickiness described as an internal power of the adhering of two neighboring lamina of a fluid and possessing properties of cohesion, or in other words, as a tangential force necessary to separate contiguous lamina of that fluid. This phenomenon weakly depends on flow velocity and a flow velocity gradient was proposed by Count Rumford in 1796 [27], and was described mathematically as pressure frictional relaxation, proposed by POISSON [28] and by NATANSON [29]. Different concepts of fluid resistance, in laminar flow, causes different hypothetical velocity profiles as presented in Fig. 1. The phenomenon of viscosity predominates when the motion is laminar (not turbulent). However, a third mode of motion, called the non-Newtonian form of internal friction, is connected with the irregular motions of molecules, and is called sinusoidal or tumultuous motion. This mode of internal friction mainly depends on the square of the velocity gradient. Finally, the internal friction of fluids, expressed mathematically by the tensor of flux of frictional resistance, should consider three different contributions:

$$(2.1) \quad \mathbf{r} = a_0(\varpi)\mathbf{I} + 2a_1\mathbf{d} + a_2\mathbf{d}^2.$$

The first part is pressure-dependent friction, the second is the Newtonian friction component proportional to the shear rate \mathbf{d} and the final part is flow-resistance dependent on the energy of shear rate. This nonlinear expression cannot be further considered within the framework of the Navier–Stokes equation, therefore PRANDTL in 1904 [30] proposed the following approximated nonlinear formula with respect to the invariance of \mathbf{d} , but tensorially linear with respect to \mathbf{d} :

$$(2.2) \quad \mathbf{r} = \left(\frac{a_0(\varpi)}{\text{III}_{\mathbf{d}}} + 2a_1(\text{I}_{\mathbf{d}}, \text{II}_{\mathbf{d}}, \text{III}_{\mathbf{d}}) + a_2(\text{I}_{\mathbf{d}}, \text{II}_{\mathbf{d}})\text{III}_{\mathbf{d}} \right) \mathbf{d}.$$

Here $\mathbf{r} = \tau_{ij}\mathbf{e}_i \otimes \mathbf{e}_j = \mathbf{r}^T$, $i, j = x, y, z$ is a symmetric tensor of frictional resistance, a_0, a_1, a_2 are, respectively, constitutive coefficients of stickiness, viscosity and tumultuousness, $\mathbf{I} = \delta_{ij}\mathbf{e}_i \otimes \mathbf{e}_j$ is Gibbs' identity tensor (Eq. (2.1)), $\mathbf{d} = \frac{1}{2}(\text{grad } \mathbf{v} + \text{grad}^T \mathbf{v}) = d_{ij}\mathbf{e}_i \otimes \mathbf{e}_j$ is a symmetric part of the velocity gradient called the Euler rate of deformation – the component $d_{xr} = \dot{\gamma}$ of this tensor is traditionally called the shear rate when the circumferentially symmetrical flow in a pipe or tube is considered. The first, second and third invariants of \mathbf{d} are denoted as $\text{I}_{\mathbf{d}}, \text{II}_{\mathbf{d}}, \text{III}_{\mathbf{d}}$, respectively.

Different hypothetical velocity profiles accounting for different concepts of fluid resistance undergoing laminar flow are collected in Fig. 1.

Similarly, flows of fluids in tubes are mainly represented only by one component of the resistance tensor: τ_{xr} called the shear stress. Especially important is

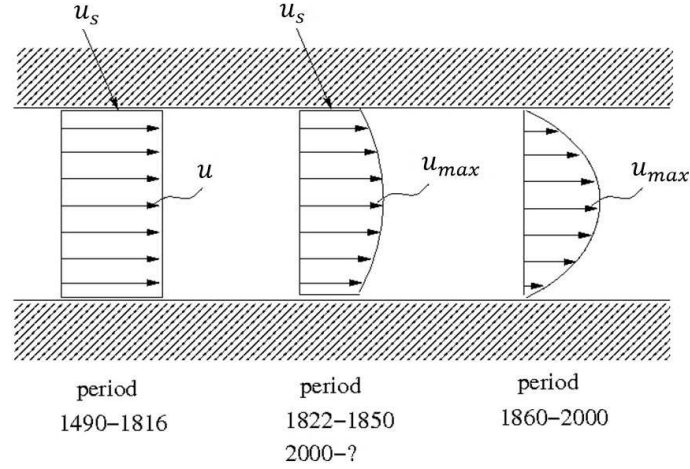


FIG. 1. Different hypothetical velocity profiles accounting for different concepts of resistance, where: u – main component of the velocity, u_s – main component of the slip velocity, u_{max} – the maximal value of u at the axis of the pipe.

the value of τ_{xr} on the solid boundary of the tube; then, according to Young's assumption, it is called the wall stress and is denoted as $\tau_w = \tau_{xr}(r = R)$. For one dimensional flow within a pipe, the constitutive formula (2.2) on the pipe wall reduces to:

$$(2.3) \quad \tau_w = \left(\frac{a_0}{|d_{xr}|} + 2a_1 + a_2|d_{xr}| \right) d_{xr}; \quad d_{xr} = \frac{1}{2} du/dr|_{r=R},$$

where the main component of the velocity along the pipe axis is $\mathbf{v} = u(r, t)\mathbf{e}_x$.

A special form of wall stress, which takes into account a turbulent viscosity coefficient, has been proposed by PRANDTL [30]:

$$(2.4) \quad \tau_w = (2\mu + \rho l_{Pr}^2 |d_{xr}|) d_{xr}.$$

In this model the wall stress depends explicitly on the distance of the layer from the surface, designated as y , since an internal scaling parameter proposed by Prandtl, today called the length of mixing, possesses the following form: $l_{Pr} = 0.4y$ [31].

A more concise proposal, which does not possess any geometrical quantities in the constitutive relations, has been proposed by von Kàrmàn:

$$(2.5) \quad l_{Ka} = 0.4 \left| \frac{\partial u}{\partial y} \right| \left| \frac{\partial^2 u}{\partial y^2} \right|^{-1},$$

where the second-order derivatives on the boundary appear. This approach directly leads to the rational modeling of turbulence by co-called high-order gradient models. Yet a more correct formula for the length of turbulent mixing has

been proposed by Novoshilov and implemented by KARCZ and BADUR [32]:

$$(2.6) \quad l_{\text{No}} = 0.4 \frac{\mu}{\rho} \left| \frac{\partial u}{\partial y} \right|^3 \left| \frac{\partial^2 u}{\partial y^2} \right|^{-1},$$

which can be simply extended into the 3D case [32].

An explicit second-order model of the wall stress can be obtained by Chapman–Enskog expansions and Burnett type approximations in the kinetic theory of gases [20]. Then, according to DEISSLER’s [18] approximation of a wall action, the second-order expression for the wall stress is [3, 33]:

$$(2.7) \quad \tau_w = A_1 Kn \frac{\partial u}{\partial y} + A_2 \frac{Kn^2}{2} \frac{\partial^2 u}{\partial y^2}.$$

Unfortunately, Eq. (2.7) can be considered only in the neighborhood of a wall. Therefore for the whole domain of fluid, a new equivalent definition of \mathbf{r} which takes into account the second-order model of stresses should be incorporated.

A well-known MAXWELL [7] proposal for the second-order definition of \mathbf{r} has been developed, as the high-order thermal gradient resistance tensor, in the form:

$$(2.8) \quad \mathbf{r} = -2\mu \mathbf{d} + \frac{2}{3}\mu \mathbf{I}_d \mathbf{I} + \beta_1 \frac{1}{2}(\text{grad } \mathbf{g} + \text{grad}^T \mathbf{g}) + \beta_2(\text{div } \mathbf{g}) \mathbf{I},$$

where $\mathbf{g} = \text{grad } \theta$ is the gradient of temperature and β_1, β_2 are the constitutive constants which can be called the internal transpiration coefficients. Additional flow resistance can also be governed by:

$$(2.9) \quad \mathbf{r} = -2\mu \mathbf{d} + \frac{2}{3}\mu \mathbf{I}_d \mathbf{I} + 2\beta_3 \mathbf{d}_{(2)},$$

where $\mathbf{d}_{(2)} = \frac{1}{2}(\text{grad } \mathbf{a} + \text{grad}^T \mathbf{a}) \neq \dot{\mathbf{d}}$ is the acceleration of deformation dyad (deformation tensor) proposed by REYNOLDS [34] or by the “double-order resistively” governed by the internal scale length l_{T_0} [32]:

$$(2.10) \quad \mathbf{r} = -2\mu(\mathbf{d} + l_{\text{T}_0}^2 \text{lap } \mathbf{d}) + \frac{2}{3}\mu(1 + l_{\text{T}_0}^2 \text{lap}) \mathbf{I}_d \mathbf{I},$$

where the Laplacian operator is: $\text{lap}(\cdot) = \text{div grad}(\cdot)$.

An interesting proposition for rebuilding the definition of the resistance tensor can be found in the paper by DONGARI *et al.* [35]. They introduced a model process dedicated to modeling of the enhanced flow of rarefied gases as well as the Knudsen paradox. By defining an additional “diffusion velocity” $\mathbf{u} = -D \text{grad}[\ln(\rho\sqrt{\theta})]$ the authors obtained the extended resistance tensor:

$$(2.11) \quad \mathbf{r} = -2\mu \mathbf{d} + \frac{2}{3}\mu \mathbf{I}_d \mathbf{I} + \beta \frac{1}{2}(\mathbf{u} \otimes \mathbf{v} + \mathbf{v} \otimes \mathbf{u}) + \gamma(\mathbf{v} \cdot \mathbf{u}) \mathbf{I},$$

where the coefficients are: $\beta = 2\rho$, $\gamma = -2/3\rho$. In comparison with Maxwell's model (2.8), which is a second-order thermal transpiration one, the above model can be considered as a first-order internal thermal transpiration. One has to notice that the model, with diffusion velocity (2.11), leads to excellent agreement with the MAURER *et al.* [13] experiments without involving any slip model.

Yet another higher-order gradient model of internal resistance, based on a notion of the "internal scale parameter" k playing a similar role as the mixing length in (2.4), can be [32]:

$$(2.12) \quad \mathbf{r} = \alpha \left\{ \frac{\rho}{2} k \mathbf{I} + \frac{1}{2} \alpha_1 k [\text{grad}(\rho \mathbf{j} + \rho \mathbf{v}) + \text{grad}^T(\rho \mathbf{j} + \rho \mathbf{v})] \right\} \\ + \frac{1}{2} \rho [(\mathbf{j} + \mathbf{v}) \otimes \text{grad} k + \text{grad} k \otimes (\mathbf{j} + \mathbf{v})],$$

where α , α_1 are phenomenological constants and turbulent mass flux is determined by the gradient of $(k)^{1/2}$; $\mathbf{j} = \alpha_1 [k^{1/2} \text{grad} \rho + \rho \text{grad}(k^{1/2})]$. An evolution equation for the parameter k [it has the same physical dimension as the turbulent kinetic energy] should be postulated separately using the Reynolds "discriminant equation". Additional complementary rational models of turbulent resistance are discussed by KARCZ and BADUR [36].

2.2. Viscosity of rarefied gases

In the literature there is known a most simple method of modeling of flow-enhanced resistance by making the viscosity a variable quantity [33, 37, 38]. This approach assumes a strong decrease (as many as 20 times) of the viscosity coefficient near the wall: $\mu_e = \mu_0 \chi^{(1-\delta)}/(C\delta)$ where δ , C are phenomenological constants and $\chi = y/\lambda$ – dimensionless distance from the wall. The slip boundary conditions are simplified for the case owing to the radical friction reduction near the wall in such models. The integration of complex numerical formulas in very thin boundary layers, which was presented in works [17, 34], is not easy, hence the radical friction reduction near the wall is a huge simplification or even an omission of sophisticated mathematical structure. But the variable viscosity coefficient is an alternative resolution to introduce the slip boundary conditions. BESKOK and KARNIADAKIS proposed a Bosanquet-type expression for the viscosity [15]:

$$(2.13) \quad \mu_e = \mu_0 \frac{1}{1 + \alpha Kn}, \quad \alpha = 2.2.$$

The purpose is to extend the slip model with dimensionless slip length [34]:

$$(2.14) \quad Na = \frac{2-f}{f} \frac{Kn}{1-bKn}, \quad b = -1,$$

from the slip-flow regime to the transition, to the free molecular regime as well.

2.3. Fluid surface friction

The second important mode of flow resistance was discovered by D’ALEMBERT in 1752 [39]. It is the external friction of fluid along the solid boundary of a surrounding canal. In the opinion of D’Alembert this mode of resistance is more important than the Newtonian one coming from internal friction of fluid lamina.

The D’Alembert hypothesis concerning the laws of external friction was mathematically expressed by COULOMB in 1801 [40] as a sum of three vectors:

$$(2.15) \quad \mathbf{f}_r = \left(\frac{\nu_0}{|\mathbf{v}_s|} + \nu_1 + \nu_2 |\mathbf{v}_s| \right) \mathbf{v}_s.$$

It means that a surface (skin) friction force \mathbf{f}_r appearing between a contacting fluid and a solid material is some additive function of powers of the slip [relative] velocity $\mathbf{v}_s = \mathbf{v}_{\text{fluid}} - \mathbf{v}_{\text{wall}}$. These are the adherence, slip and kinetic parts. Precisely, due to assumed isotropy of friction, the direction of the vector of friction force and the adherence part vector part are parallel to themselves and identical with the direction of the slip velocity. In the case of patterned roughness of the wall, in general, the isotropic coefficients ν_0, ν_1, ν_2 become the symmetric friction tensors which possess dimensions of matrix 2×2 [41].

From the historical point of view, the skin (surface) friction force (2.3) is connected with the problem of resistance in elastic fluids (see: the first velocity profile in Fig. 1). According to Euler, by elastic fluid one understood such fluids as air and other gases where internal resistance had to be omitted; therefore, in the elastic fluid any resistance can appear only between solid and fluid materials. Analyzing air resistance, researchers such as Galileo, Marriotte, Picard and Cassini [42] had assumed that resistance is proportional to the square of velocity, in that time called the *vis viva*. But, finally, Huygens, circa 1670, had deduced the law that the air resistance is proportional to the square of fluid velocity. It appears that third part in (2.15), historically, was first taken into account by researchers. In his celebrated monograph D’ALEMBERT [39] discussed, but separately, three contributions to the skin friction. It was de Saint-Venant in 1887 [43], who interpreted a kinetic part of a skin friction as a force which separates the “skin eddies” from the fluid-solid contacting layer.

For the first time, the adherence component was considered analytically by DUHEM in 1903 [44] who discussed required values of the coefficient ν_0 . The second coefficient of linear skin friction $\nu_1 = \nu$ had been used by many researchers before Navier, but it was indeed due to Navier’s unique efforts that the two mechanisms of resistance – the internal one (governed by viscosity μ) and the external one (governed by surface viscosity ν) – had appeared in one concise mathematical model (see: the middle profile in Fig. 1). Let us note that in the

time of Navier, it was difficult to measure an internal fluid viscosity μ . NAVIER in 1827 [45], in the end, simplified his analytical solution, removing μ and giving a formula for a mass flow rate in a pipe only in terms of external viscosity ν . His first constitutive expression for the coefficient ν between water and glass had been based on Gérard's experiments and originally reads: " $\nu = 0.3333\rho$ " [45].

For one-dimensional pipe flow the friction force acts only along the pipe axis: i.e. $\mathbf{f}_r = f_r \mathbf{e}_x$, and this main component is:

$$(2.16) \quad f_r = \left(\frac{\nu_0}{|u_s|} + \nu_1 + \nu_2 |u_s| \right) u_s,$$

where u_s is the main component of $\mathbf{v}_s = \mathbf{v}_{\text{fluid}} - \mathbf{v}_{\text{wall}} = u_s \mathbf{e}_x$. In the literature only one linear $\nu_1 \equiv \nu$ (or slip) coefficient has been employed and is usually numerically and experimentally determined. In practice, the ratio $\mu/\nu = l_s$, called the slip length has been evaluated and measured in a variety of experiments (see [21]). It should be highlighted that Helmholtz and Piotrowski, in 1860, defined a ratio $\mu/\nu = l_s$ as the slip length, and its dimensionless value is called the Navier number and should be defined by the following formula:

$$(2.17) \quad Na = \frac{l_s}{d},$$

where d is a characteristic dimension of the channel [16, 34, 46, 47]. The importance of the dimensionless slip length (the Navier number) Na is considered in the next section.

3. Dimensionless friction numbers

Traditionally, the most important of dimensionless numbers in fluid dynamics are considered for the momentum governing equations. The balance of momentum undergoes of a sort of purely mathematical analysis in a so-called dimensionless form. A fundamental and widely-known dimensionless number related to viscosity and insertion force is the Reynolds number:

$$(3.1) \quad Re = \frac{\dot{m} d_n}{A \mu}$$

which also can be understood as a dimensionless mass flow rate \dot{m} , where d_n is the hydraulic diameter and A is the cross section of the channel. Since for many flows, viscosity μ weakly depends on the temperature and pressure, and hence, $\dot{m}_{\text{in}} = \dot{m}_{\text{out}}$, the Reynolds number can be interpreted as a total (integral) flow parameter. One should remember that in the above definition the mass flow rate is defined via the normal component of velocity $u_n = \mathbf{v} \cdot \mathbf{n}$, which usually is

less than the velocity length $c = |\mathbf{v}| > u_n$. For open canals, where cannot be determined, Re usually means dimensionless inflow velocity u_∞ [16, 34, 47].

To answer the question stated in the introduction the Stanton and Pannell contribution to resistant force should now be presented. STANTON and PANNELL [48], making measurements of water flow within a capillary pipe, proposed a change of the paradigm in the approach to the description of flow characteristics. They had the courage to describe the results of measurements in a quite new way – they broke away from the celebrated pressure-discharge characteristics “ $\Delta p - \dot{m}$ ”, deciding to present their own results as the diagram “Dimensionless Wall Stress – Dimensionless Mass Flow Rate”. The dimensionless wall stress, referred to as the Stanton–Pannell friction factor, was defined as the wall stress divided by the *vis viva* of the flow: $f_{SP} = \tau_w/(\rho u^2)$. The dimensionless mass flow rate was defined as the Reynolds number following Eq. (3.1). In the considered cases the “ $f_{SP} - Re$ ” characteristics of the analytical solutions of the one-dimensional Navier–Stokes equation can be identified by the following equation [16]:

$$(3.2) \quad f_{SP} = \frac{\tau_w}{\rho u^2} = \begin{cases} \frac{4\mu}{d\rho u} = \frac{8}{Re} & \text{no-slip solution,} \\ \frac{4\mu}{d\rho u(1 + 4l_s/d)} = \frac{8}{Re(1 + 4Na)} & \text{slip solution.} \end{cases}$$

In the contemporary literature, instead of “*vis viva*”, we use “kinetic energy” which is two-times less in quantity, and such obtained dimensionless wall stress is called the Fanning friction factor: $f_F = 2f_{SP}$. Frequently, according to Darcy, we apply a four times greater coefficient, called the Darcy friction factor $f_D = 4f_F = 8f_{SP}$ [4, 16]; it leads to the well-known expression: $f_D = 64/Re$.

In the laminar regime, the classical no-slip Hagen–Poiseuille solution $f_D = 64/Re$ and the slip Helmholtz–Piotrowski solution $f_D = 64/Re(1 + 4Na)$ are plotted. In the turbulent regime for smooth pipes, the no-slip Blasius solution $f_D = 0.316 Re^{-0.25}$ is plotted as continuous lines. Some experimental results [22] for flow of gas within a peek-coated, fused-silica microchannel is also shown. The friction factor is reduced due to slip at the walls as $f_{SP-slip}/f_{SP-no-slip} = 1/(1 + 4Na)$ [49]. One crucial element of $f_D - Re$ universality is the appearance of a single critical point exactly at the same level of viscosity and inertia forces proportion. It should be mentioned that this point appears on the “ $\Delta p - \dot{m}$ ” diagram, as well as in the classical literature by Du Buat, Prony, Darcy, Eytelwein where also exists some qualitative information about “transition” from a quiet form of flow into a loud one. Finally, Reynolds, in the case of a pipe, found a critical number for the laminar-turbulence transmission as: $Re_{cr} = 2300$.

Furthermore, for uniquely expressing a critical point on a plane of $f_D - Re$ two coordinates are needed. The second critical coordinate has been discovered

by STANTON and PANNELL [48] as follows:

$$(3.3) \quad \begin{aligned} Re &= \frac{\rho u_{cr} d}{\mu} \quad \text{is constant } \sim 2300, \\ StPa &= \frac{\rho d^3}{\mu^2} \frac{dp}{dx|_{cr}} \quad \text{is constant } \sim 0.004. \end{aligned}$$

The Stanton–Pannell number $StPa$ depends only on a drop of pressure and can give useful information such as the resistance of a system at the design level or the calibration of new channels on the basis of experimental measurements. This number is connected with another dimensionless factor called the Poiseuille number $Po = f_D \cdot Re$ of the following form:

$$(3.4) \quad StPa = \frac{1}{2} Po Re = \frac{1}{2} f_D (Re)^2.$$

From Eq. (3.2) it follows that the critical Darcy friction factor always is: $f_D = 0.32$.

Enhancement of the Poiseuille number due to slip is $Po_{slip}/Po_{no-slip} = 1/(1 + 4Na)$. This result is consistent with [22] where, for square channels, they have obtained: $f_D \cdot Re = 56.9/(1 + 7.88Kn)$. It should be highlighted that due to the fact that the phenomenon of the laminas-to-turbulent transition does not occur simultaneously in the entire channel, in practice, we are speaking of the “transition region” [1, 2], which has been evidenced in Fig. 2.

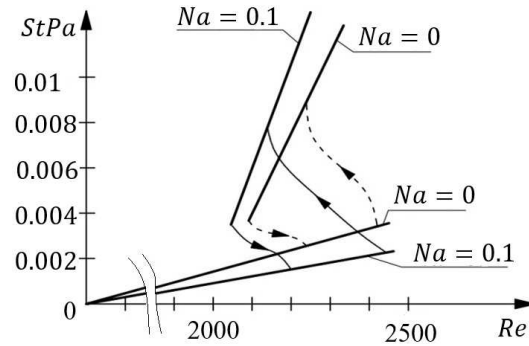


FIG. 2. Dimensionless characteristic of the Stanton–Pannell number $StPa$ and Reynolds number Re including scale effect by the Navier number Na [16].

In Fig. 2 the wall stress τ_w [treated as a surface friction force per unit area] is replaced by means of an analytical solution to the measurable fall of pressure dp/dx . Thus, practically, the Darcy friction factor f_D has the same information that is described by the Stanton–Pannell number: $StPa$. Dependence of the

Stanton–Pannell number $StPa$ on the Navier number Na and Reynolds number Re suggests the answer that friction is also dependent on the scale effect. Figure 2 is obtained on the basis both the MORINI *et al.* and CELATA *et al.* measurements [1, 4, 22] and analytical consideration [16].

Stanton and Pannell were the first experimentalists who believed in a theoretical anticipation of different profiles of fluid velocity within a pipe cross section. Therefore they tried to measure two kinds of velocities – the first, the classical da Vinci mass velocity, measured by weight of the total discharge of a fluid passing through a pipe section within the given time frame. The second one is the maximum velocity at the axis of the pipe, estimated by measuring the pressure difference between that in a small Pitot tube located at the axis of the pipe facing the current and that in a small hole in the wall of the pipe. As we know from basic examination, this pressure difference is $\frac{1}{2}\rho u_{\max}^2$ and from this relation the maximum velocity [speed] can be calculated. Everyone involved was profoundly astonished by a plot of the velocity ratio $\varphi_{SP} = u/u_{\max}$ that had been made for different falls of pressure, expressed as a logarithm of the dimensionless [Reynolds] number. Prior studies available in the literature have paid no attention to the issue of the Stanton–Pannell critical number during laminar to turbulent transition [1]. With respect to nanochannels, the notion of the Reynolds number and the Stanton–Pannell number is meaningless and should be replaced by the Navier number. Additionally, the role of the Navier number leads to expressing flow enhancement in the laminar-turbulent transition regime [16, 50, 51].

4. Maxwell kinetic theory within a boundary layer

As discussed here, the MAXWELL’s paper, entitled “*On stresses in rarified gases arising from inequalities of temperature*” [7], possesses two distinct parts, based on two strongly independent motivations. The first part of the paper, called here “March 1878”, is motivated by an attempt to explain CROOKES’ discovery of the rotation of a “windmill” in a partially evacuated radiometer [52]. Maxwell put forth a basic hypothesis that, in Crookes’ experiments, since the pressure is very low, the new stresses are growing due to a second gradient of temperature in the rarefied gas. These stresses are capable of producing rapid motion in a radiometer windmill. In other words, in gaseous medium where there is only a linear distribution of temperature, there are no additional thermal stresses. A problem of boundary conditions in this first part of a paper [from March 1878] was not considered.

But, in that time, Maxwell was conscious that this kind of thermal stress, calculated for a hot solid sphere of uniform temperature immersed in a colder gas, cannot itself give rise to any force tending to move the sphere in one direction rather than in another. In the framework of his model of stresses, the

sphere placed within the finite portion of gas is already in equilibrium. How then to account for the fact observed by TYNDALL, that an additional force acts between solid bodies immersed in rarefied gases [53]. This kind of motion, nowadays called *thermophoresis*, is connected with small solid particles, typically spherical, suspended in a fluid within which an externally imposed linear temperature difference [constant temperature gradient] induces a force that moves the sphere from the hotter to the colder place, that is, the particle moves against the temperature gradient [54].

In order to explain this, even in March 1878, Maxwell turned his attention not to his own model of thermal stresses but to slip phenomena discovered in liquids by HELMHOLTZ and PIOTROWSKI [55] and KUNDT and WARBURG [56] in rarefied gases. The mechanical slip phenomenon is related to the finite value of the Navier external viscosity and appears as a sliding of a fluid in contact with the surface of a solid. Maxwell precisely underlined a difficulty of mathematical treatment, since the gas close to the solid surface is probably in a quite different “state of condensation” – which means that a quite different model is needed for describing the phenomena of sliding. One example of this extraordinary situation, discovered by KUNDT and WARBURG [56], is the fact that the velocity of sliding of the gas over the surface, induced by given tangential viscous stresses, varies inversely as the pressure.

In the first part (March, 1878) of his celebrated paper MAXWELL [7], did not attempt to take into account the effect of this mechanical sliding motion, because the main goal of his paper was devoted to the introduction of a thermal stress model in the bulk – consideration of a kinetic relation close to the solid surface that would be “completely destroying the simplicity of our first solution to the problem”.

4.1. Maxwell’s model of the thermal transpiration in the bulk

Let us now very briefly recapitulate the Maxwell results concerning an additional stress related to “inequalities of temperature”. These stresses can only appear when the field of temperature is nonlinear. Maxwell has proposed the following constitutive formula [7]:

$$(4.1) \quad \mathbf{p} = p\mathbf{I} - 2\mu\mathbf{d} + \frac{2}{3}\mu\mathbf{I}_d\mathbf{I} + \beta_1\frac{1}{2}(\text{grad } \mathbf{g} + \text{grad}^T \mathbf{g}) + \beta_2(\text{div } \mathbf{g})\mathbf{I},$$

where $\mathbf{p} = p_{ij}\mathbf{e}_i \otimes \mathbf{e}_j = \mathbf{p}^T$ is bulk flux of momentum, the temperature gradient is denoted as $\mathbf{g} = \text{grad } \theta$ and β_1, β_2 are the constitutive constants which can be called the bulk thermal transpiration coefficients (see also Eq. (2.8)).

After substitution of the above equation for the balance of momentum and after using a few tensorial identities: $\text{grad } \mathbf{g} = \text{grad}^T \mathbf{g} = \theta_{ij}, \mathbf{e}_i \otimes \mathbf{e}_j, \text{div } \mathbf{d} =$

$\frac{1}{2}\{\text{lap } \mathbf{v} + \text{grad } I_{\mathbf{d}}\}$, we obtain an equation of fluid motion that takes into account the above defined unconventional bulk thermal transpiration contribution to the momentum transport:

$$(4.2) \quad \rho \dot{\mathbf{v}} + \text{grad } p - \mu \text{lap } \mathbf{v} + \frac{1}{3} \text{grad } I_{\mathbf{d}} + \beta_1 \text{lap } \mathbf{g} + \beta_2 \text{grad}(\text{div } \mathbf{g}) = \rho \mathbf{b}.$$

If Maxwell's constitutive constants β_1 and β_2 are vanishing to zero, the model of the fluid under consideration becomes identical to the Stokes model of viscous compressible fluid [47]. Further taking the following identities: $\text{div } \mathbf{g} = \text{lap } \theta$ and $\text{lap } \mathbf{g} = \text{lap}(\text{grad } \theta) = \text{grad}(\text{lap } \theta)$ we write (4.2) to be:

$$(4.3) \quad \rho \dot{\mathbf{v}} + \text{grad } p - \mu \text{lap } \mathbf{v} + \frac{1}{3} \text{grad } I_{\mathbf{d}} + (\beta_1 + \beta_2) \text{grad}(\text{lap } \mathbf{g}) = \rho \mathbf{b}.$$

Utilizing the non-equilibrium kinetic treatment, Maxwell was able to estimate the value of the thermal transpirations constants to be [7]:

$$(4.4) \quad \beta_1 = 3 \frac{\mu^2}{\rho \theta}, \quad \beta_2 = \frac{3}{2} \frac{\mu^2}{\rho \theta}.$$

These are really very small quantities that depend on viscosity μ , density of the gas ρ , and its' temperature θ . Let us note that making more concise calculations with the Maxwell fundamental equation, which considers also its nonlinear components, one can obtain the expression for the stress tensor in thermal transpiration phenomena which depends additionally on a linear distribution of temperature [57]:

$$(4.5) \quad \mathbf{p} = p \mathbf{I} - 2\mu \mathbf{d} + \frac{2}{3} \mu I_{\mathbf{d}} \mathbf{I} + \beta_1 \frac{1}{2} (\text{grad } \mathbf{g} + \text{grad}^T \mathbf{g}) + \beta_2 (\text{div } \mathbf{g}) \mathbf{I} + \beta_3 \mathbf{g} \otimes \mathbf{g}.$$

But it should be noted from the very beginning that a boundary condition, where the coefficient β_3 and the first gradient of temperature \mathbf{g} appears, is fundamentally quite different from Maxwell's original example, since \mathbf{g} appears within the mobility force \mathbf{f}_m which physically suggests another phenomena. It is also a historical truth that the presence of \mathbf{g} in the boundary layer was first postulated by REYNOLDS [5] and later proven by MAXWELL [7].

4.2. Maxwell's model of thermal transpiration within a slip layer

Let us now consider the second part of Maxwell's paper, known as "Appendix May 1879" [few months before Maxwell death]. His direct reason for writing this appendix was the important Reynolds' discovery of thermal transpiration. Maxwell, having been a reviewer of REYNOLDS seminal paper [5], had an occasion to study all Reynolds' eight laws of thermal transpiration, though early as a manuscript, before its' formal publication. The thing of great novelty was

Reynolds' proposal for the modeling of thermal transpiration, i.e. the motion of gas from the colder to hotter ends, through a capillary thin porous plate of which the sides undergo different temperatures. Reynolds was able to predict the transport of momentum as one-dimensional steady-state momentum drift between the hot and cold reservoirs, situated at opposite ends of the porous plate, with the resulting constant local temperature gradient at each point of the fluid being in an isobaric state.

As it happens that these conditions are quite in opposition to the Maxwell bulk model of stresses Eq. (4.1) – here there is only a linear distribution of temperature – the only approach is to turn to boundary slip phenomena, where a boundary force must be postulated that depends on a thermal gradient. This concept, proposed early in REYNOLDS' manuscript [5], is a subject of MAXWELL'S celebrated appendix [7].

Maxwell assumes, having Reynolds' solution in hand, that the kinetic theory of gases close to a solid surface should be reformulated and the governing equations should take on the conditions which must be satisfied at the surface of solid body. Unfortunately, his solid body surface is absolutely rigid and in a stress-free state; its molecules are absolutely fixed which means that the surface temperature is nearly absolute zero.

In turn, using the expression for the fluid stress tensor from the Stokes boundary condition:

$$(4.6) \quad \operatorname{div}_s(\gamma \mathbf{I}_s) - \varpi \mathbf{n} + \mathbf{f}_{\partial V} + \mathbf{p} \mathbf{n} = 0,$$

where the Young–Laplace surface tension is $\mathbf{p}_s = \gamma \mathbf{I}_s$, the general form of boundary forces, that consist of contributions from the friction and the mobility components $\mathbf{f}_{\partial V} = \mathbf{f}_r + \mathbf{f}_m$, the surface Gibbs identity is defined to be: $\mathbf{I}_s = \mathbf{I} - \mathbf{n} \otimes \mathbf{n}$ and \mathbf{n} is the unit normal vector on the boundary surface and ϖ is the Stokes normal surface pressure. It is assumed that at the boundary of the layer the usual spherical pressure tensor changes into an ellipsoidal pressure tensor, and it follows that we would obtain a boundary relation of this same sort. Surface divergence div_s is defined as a right contraction of the surface gradient [25]: $\operatorname{grad}_s(\cdot) = \operatorname{grad}(\cdot) \mathbf{I}_s$.

The difference of the Maxwell approach in the contact of two gasses, for instance hydrogen and CO₂, with the same glass surface is only in the number of absorbed and reflected gas molecules. Maxwell prefers to treat the surface as something intermediate between a perfectly reflecting and a perfectly absorbing surface. Therefore, an experimentally verified portion f describes the absorption of all the incident molecules, and the portion $1 - f$ describes the perfect reflection all molecules incident upon it.

Finally, Maxwell obtains the following boundary conditions. Let us suppose that the surface is a plane y, z and that the gas flowing on that side of it for

which x is positive. Let u_s be a main surface component of velocity in the main y direction, then the slip velocity formula is given by the following expression:

$$(4.7) \quad u_s - G \left(\frac{du}{dx} - \frac{3}{2} \frac{\mu}{\rho\theta} \frac{d^2\theta}{dx dy} \right) - \frac{3}{4} \frac{\mu}{\rho\theta} \frac{d\theta}{dy} = 0,$$

where G is the Helmholtz–Piotrowski slip length, μ internal viscosity coefficient, ρ – gas density, θ – absolute temperature. To bring to fruition the process of reconstruction of the Maxwell slip boundary condition (4.7), let this boundary condition be treated as a Stokes force condition (4.6). Thus, the elements of (4.7) have the representation:

- the fluid wall stress:

$$(4.8) \quad \mathbf{pn} = \left\{ p\mathbf{I} - 2\mu \mathbf{d} + \frac{2}{3}\mu \mathbf{I}_d \mathbf{I} + \beta_1 \frac{1}{2}(\text{grad } \mathbf{g} + \text{grad}^T \mathbf{g}) + \beta_2(\text{div } \mathbf{g}) \mathbf{I} \right\} \mathbf{n},$$

- the surface friction force:

$$(4.9) \quad \mathbf{f}_r = \nu(\mathbf{v} - \mathbf{v}_{\text{wall}}),$$

- the surface mobility force:

$$(4.10) \quad \mathbf{f}_m = -c_{m\theta} \text{grad}_s \theta.$$

The thermo-mobility coefficient $c_{m\theta}$ should be stated, based on Maxwell’s formula (4.7), as a coefficient which is independent of the property of the solid surface:

$$(4.11) \quad c_{m\theta} = \frac{3}{4} \frac{\mu\nu}{\rho\theta}.$$

Next, using definition $l_s \equiv G = \mu/\nu$, after dividing the balance (4.6) by ν we obtain a generalization of the Maxwell slip boundary layer (4.7) as:

$$(4.12) \quad \mathbf{v} - \mathbf{v}_{\text{wall}} - \frac{c_{m\theta}}{\nu} \text{grad}_s \theta + \frac{p - \varpi}{\nu} \mathbf{n} - 2l_s \mathbf{dn} + \frac{2}{3} l_s \mathbf{I}_d \mathbf{n} + \frac{\beta_1}{\nu} \frac{1}{2} (\text{grad } \mathbf{g} + \text{grad}^T \mathbf{g}) \mathbf{n} + \frac{\beta_2}{\nu} (\text{div } \mathbf{g}) \mathbf{n} = 0.$$

In analogy, the ratios $l_{s\beta_1} = \beta_1/\nu$, $l_{s\beta_2} = \beta_2/\nu$ can be called the thermal transpiration slip coefficients. From the above, we conclude that $l_s = \mu/\nu$ cannot be treated as only one characteristics of the Navier–Stokes layer, but undoubtedly it is a main characteristic of the external viscosity.

Finally, if one introduces, following Maxwell, a directional derivative “ d/ds ”, directed along some main flow direction “ \mathbf{t} ” with the cosines given by l , m , n , then the condition (4.7) can be expressed in the original form [7]:

$$(4.13) \quad \mathbf{v} - l_s \frac{d}{ds} [(1 - \mathbf{t}^2) \mathbf{v} - (\mathbf{t} \times \mathbf{v})(\mathbf{t} \otimes \mathbf{t})] + l_s \beta_2 \mathbf{t} \frac{d}{ds} \left(\frac{d\theta}{ds} \right) - \frac{c_{m\theta}}{\nu} \text{grad}_s \theta = 0.$$

This equation is called the “*Maxwell slip boundary layer equation*”. Let us note that in each component of this equation, the gradient of temperature plays a very special role. It is a completely external surface effect which is not connected with the form of stress tensor, for instance with Eq. (4.5). This means that the motion of gas close to a solid surface, in general, is governed by two kinds of forces. The first is a mechanical friction force, connected with the external viscosity, and the second one is a temperature gradient which urges gas particles closer to the surface, from colder to hotter parts of the surface. Therefore the coefficient of thermal mobility $c_{m\theta}$ [see: Eq. (4.11)] is independent of mechanical layer properties and should be experimentally verified. There are numerous modern references in the literature describing the proper experiments. The impressive electrokinetic properties predicted for carbon nano-tube channels have not yet been measured by careful experiment [8, 58, 59].

In a particular case, when a rigid cold particle is immersed into a gas at rest $\mathbf{v} \equiv 0$, putting the linearity of temperature distribution ($\text{grad } \theta = 0$), from Eq. (4.12) we obtain the thermal velocity of a particle:

$$(4.14) \quad \mathbf{U} = \mathbf{v}_{\text{wall}} = -\frac{c_{m\theta}}{\nu} \text{grad}_s \theta.$$

The velocity \mathbf{U} is nowadays called the thermophoretic velocity [60]. It characterizes the motion of nano-particles that follow from the surface gradient of temperature.

4.3. Maxwell’s closure for the Navier number

It is important that owing to application of the Kinetic Theory, Maxwell was able to find an explicit formula for the length of slipping [7]:

$$(4.15) \quad l_s = \frac{\mu}{\nu} = \frac{1}{2} \mu (2\pi)^{1/2} (p\rho)^{-1/2} \left(\frac{2}{f} - 1 \right) = \frac{2}{3} \left(\frac{2}{f} - 1 \right) l,$$

where l means the Meyer relation of the mean-free path of a gas molecule and f being the fraction absorbed. When $f = 1/2$ or the surface acts as if it were half perfectly reflecting and half perfectly absorbent then we get $l_s = 2l$. If it were wholly absorbent, $l_s = 2/3l$. In practice the slip length depends on the kind of surface and gas – for instance from KUNDT and WARBURG [56] experimental data it follows that for air on a glass surface at 17°C: $l_s = 8/p$ and for hydrogen on glass: $l_s = 15/p$, where the pressure is given in dynes per square centimeter.

In contemporary literature the coefficient of partial absorption f is called “*The Tangential Momentum Accommodation Coefficient*” (TMAC). This coefficient is not dependent on heat flow, and accounts for the average tangential to a surface momentum exchange between the fluid molecules and the solid

molecules. Its value should be evaluated experimentally, but it is known that it varies from zero (for secular reflection) up to unity (for complete or diffuse accommodation) [8, 60].

Unfortunately, the second coefficient of the Maxwell model, i.e. the coefficient of thermal mobility $c_{m\theta}$, essential for thermal transpiration, was omitted from any literature discussion. Indeed, it is defined by Eq. (4.11), since it is a combination of the bulk and of the surface properties, exactly the Navier external viscosity ν . Notice that it is a quite opposite situation within the Reynolds boundary layer model, where REYNOLDS gives a much more correct definition of the thermal mobility coefficient and a less assumptive definition of the slip length [5, 6, 61].

4.4. Implementation of a model of a boundary layer with thermal mobility

The consistency of field equations of fluid in the bulk and within the layer boundary began with REYNOLDS work [6], and this consistency has been expanded by many types of research [62–70]. Despite the fact that investigation into thermal transpiration began long ago (see: [5–7, 62, 66, 67]) many questions continue to be unanswered. This is connected with a special feature of thermal transpiration, that is very sensitive to the kind of solid material and the kind of rarefied gas. The thermal mobility force expressed by Eq. (4.10) [7], as well as proposals by REYNOLDS [6], is in general sensitive to the properties of both gas and solid surfaces and depends on two thermal momentum accommodation coefficients f_3, f_4 . However, having a complete experimental dataset, for instance the works of different authors ROJAS-CÁRDENAS *et al.* [68] PITAKARNNOP *et al.* [23], enables the development of a consistent closure to the $c_{m\theta}$ coefficient within the framework of continuum modelling.

The new benchmark experiment [68], which has applied an original method for thermal transpiration, induced mass flow rate measurements, conducted via measuring *in situ* the pressure evolution in real time at both ends of the tube using two high-speed response pressure gauges. A long, circular cross-section, glass (borosilicate) microtube ($d = 490 \mu\text{m}$; $L = 3.053 \text{ cm}$) is connected between two reservoirs: cold (no 1, environmental temperature) and hot (no 2, $\theta_2 = 80^\circ\text{C}$, heated by an internal heater) (Fig. 3) with the volume of the two reservoirs $V_H/V_C = 0.81$ and for numerical simulations $V_1 = V_C = 14.85 \text{ cm}^3$ was selected. Before experiment begins, the pressure inside the both reservoirs is regulated by means of a vacuum system and stays between 13.3 and 1330 Pa for helium. After the opening of the isolation valve, the flow induced by thermal transpiration is simple – the pressures in both reservoirs are equal and flow from cold to hot areas and is derived only by the wall mobility force (4.10), which depends on the $c_{m\theta}$ value between glass and helium and the wall temperature gradient. The volume

of the reservoirs under consideration are finite. There is presented in Fig. 3 that due to thermal transpiration gas molecules migrate from cold to hot reservoirs. As the results of this migration pressure in the cold areas decreases and at the hot areas increases.

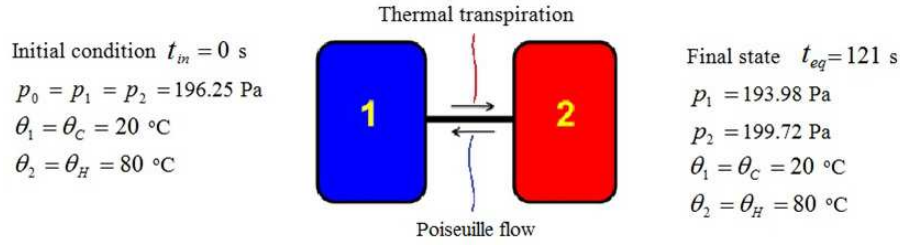


FIG. 3. Scheme of helium flow cold (1) to hot (2) reservoir [68], where initial condition: environmental temperature (cold, no 1) and $\theta_2 = 80^\circ\text{C}$ (hot, no 2) and pressure $p_1 = p_2 = p_0 = 196.25$ Pa for $t_0 = t_{in}$.

Considering the previous literature according to [16, 17, 34, 47, 50], and keeping in mind the value of the thermal accommodation coefficient proposed in the literature [61, 69], there has been made a calibration of the $c_{m\theta}$ value. Drawing from the ROJAS-CÁRDENAS *et al.* data [68] and EWART *et al.*'s considerations [70], this coefficient has been found to have the following form:

$$(4.16) \quad c_{m\theta} = \frac{3}{4} \frac{\mu^2}{\rho\theta l_s}.$$

Here the main unknown is the Navier slip viscosity ν that can also be defined by slip length (BADUR *et al.*, 2015). It was assumed that the numerical value of $c_{m\theta}$ has been calculated using the definition of the Helmholtz–Piotrowski slip length: $l_s \equiv G = \mu/\nu$, and helium-glass slip length $l_s = 0.00016$ cm. In Eq. (4.16) the temperature along the micro-pipe was taken according to linear distribution.

For the unsteady state flow analysis the Computational Fluid Dynamics (CFD) solver was employed. This finite volume based code permits one to solve three-dimensional fluid and heat flow problems involving turbulent structures and chemical reactions. However, it also allows for the addition of user-defined subroutines programmed in C++ for problems that fall outside the capability of the standard version of the code. For the implemented thermal transpiration and slip velocity condition at the wall, the numerical results agree very well with the experimental data for the pressure plots in Fig. 4. Other results of non-stationary thermal transpiration modelling of the benchmark experiment [68] with the thermal transpiration mobility force (4.10) and closure for the thermal momentum accommodation coefficient (4.16) have been presented in Figs. 5 and 6. A plot of the mass flow rate has been shown in Fig. 5 with velocity profiles for two characteristic times: of the maximum flow rate t_{\max} and zero flow rate t_{eq} (Fig. 6).

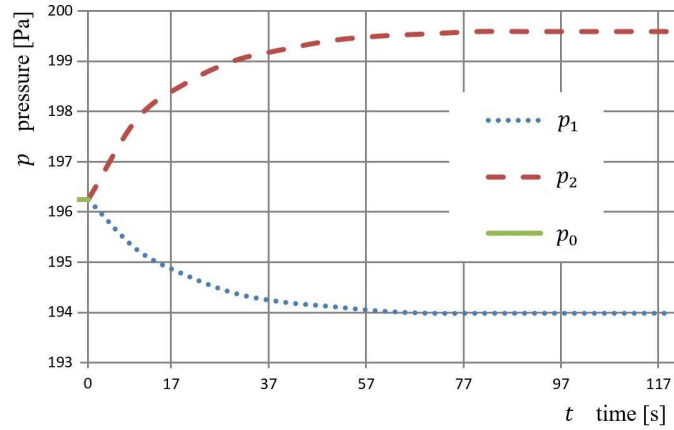


FIG. 4. Plot of pressure change in the cold (1) and hot (2) reservoirs, where initial pressure $p_0 = 196.25$ Pa for $t_0 = t_{in}$. From ZIÓŁKOWSKI and BADUR [61].

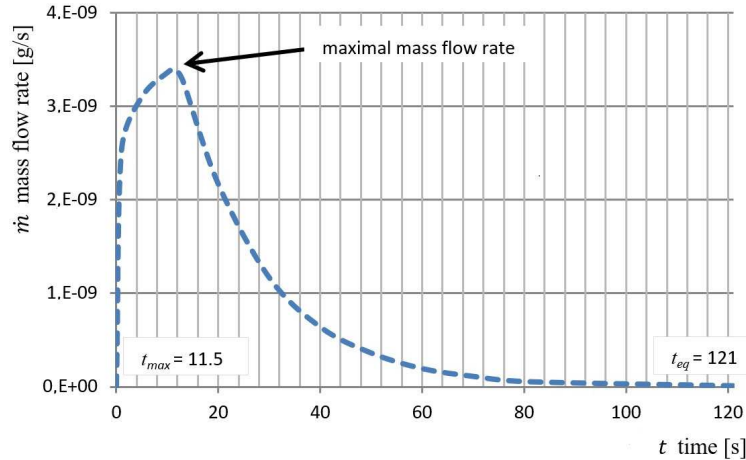


FIG. 5. Plot of mass flow rate with two characteristic times, namely: $t_{max} = 11.5$ s time of maximum flow rate and $t_{eq} = 121$ s time of zero flow rate – equilibrium conditions. From ZIÓŁKOWSKI and BADUR [61].

The mode of gas motion, driven by the difference of pressure $\Delta p = p_H - p_C$, is similar to Poiseuille's flow (see: the right side profile in Fig. 1) with a velocity profile quite opposite to that of the flow induced by (4.10), which, at the central axis, takes a maximum and is zero on the wall surface. Now, there is a characteristic time t_{max} where the thermal transpiration forces achieve maximal impact into fluid value and therefore the maximal value of mass flow rate is attained (Fig. 5). After that the Poiseuille flow governed by a difference of pressure (Fig. 4) is included, which finally leads, after time t_{eq} , to an equilibrated state when the pressure difference arrives at its maximum and the resulting mass flow rate is

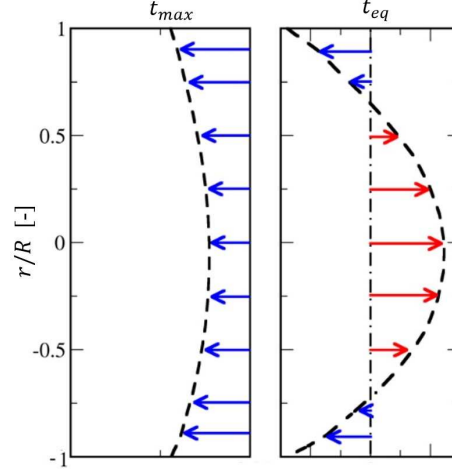


FIG. 6. Velocity profiles for two characteristic times, namely: $t_{\max} = 11.5$ s time of maximum flow rate and $t_{eq} = 121$ s time of zero flow rate – equilibrium conditions $\dot{m} = 0$ g/s; where $R = d/2$ is a radius of microtube and r is a distance from the centre of microtube.

zero. In the case of the ROJAS-CÁRDENAS *et al.* benchmark experiment [68], the following values from numerical simulations were obtained: $t_{\max} = 11.5$ s and $t_{eq} = 121$ s, respectively.

Also, during numerical simulations [61], it has been observed that the pressure variations inside both reservoirs are not perfectly mirror-symmetric with respect to the initial pressure axis, since the volumes of the two reservoirs differ (the hot is smaller). Consequentially, the pressure variation in time within the reservoirs is different – the increase in the hot (2) reservoir is to 199.72 Pa and decrease in the cold (1) reservoir is to 193.98 Pa (Figs. 3 and 4).

After implementation of the mobility force (4.10) into the commercial code, the benchmark experiment [68] has been performed for basic data corresponding to helium. For the numerical simulation it utilizes the following data: initial pressure $p_0 = p_{in} = 196.25$ Pa, cold temperature $\theta_C = 20^\circ\text{C}$, hot temperature $\theta_H = 80^\circ\text{C}$ (with linear distribution along the micro-pipe), referential viscosity $\mu = 1.96 \times 10^{-5}$ Pas, individual gas constant $\tilde{R} = 2077$ J/kg·K, and the ratio of specific heats $\kappa = 1.667$.

Pressure values are in agreement when compared with the experiment [68]. It is easy to numerically prove that at the final equilibrium zero-flow state (see Fig. 6, $t_{eq} = 121$ s) there is a connection between the Poiseuille flow in the centre of channel and counter thermal transpiration flow on the surface [61]. Hence, based on the presented model and implemented experiment a concept of Reynolds transpiration number can be proposed as follows:

$$(4.17) \quad Re t = \frac{\text{surface thermal mobility force}}{\text{volume viscous force}}.$$

5. The mystery of second-order boundary conditions

DEISSLER [18], on the basis of kinetic theory, has proposed a slip velocity equation where the second and higher derivatives of gas velocities take part [18]. It can be, in short, written as [3]:

$$(5.1) \quad \nu(\mathbf{v} - \mathbf{v}_{\text{wall}}) = \mu \left[A_1 Kn \frac{\partial \mathbf{v}}{\partial \mathbf{n}} + A_2 Kn^2 \frac{\partial^2 \mathbf{v}}{\partial \mathbf{n}^2} + \dots \right].$$

The term argued that a higher-order of the Kn and higher-order derivatives of velocity must be used in the slip equations. But on the other hand, well known kinetic theory models of fluid stress presented in work [71], do not include any contribution of a second velocity gradient – probably the Reynolds non-explicit contribution via the gradient of acceleration $\mathbf{d}_{(2)}$ (see: Eq. (2.9)) is consistent with physical interpretation. In other words, the part of wall stresses governed by the coefficient A_2 in (5.1) do make any sense from the point of view of 3D modeling.

In general, the consistency of the field equation within the bulk and on its boundary for weakly-nonlocal continua with higher gradient has not been completely solved and there are no appropriate scientific tools for solving this mathematically concise system of equations. The one known and recognized method is the so-called “Green Transformation”, by which using an extended definition of divergence, one can find the true interrelation between the bulk and the boundary equations. For instance, when a continuum description contains time derivative of the rate of deformation $\dot{\mathbf{d}}$ and its gradient $\text{grad } \dot{\mathbf{d}}$, it is simple to show, using two cycles of the Green transformation that the balance of momentum takes the Skiba–Pearson form:

$$(5.2) \quad \rho \frac{d}{dt} \left[\mathbf{v} - \text{div} \left(\frac{\partial \phi}{\partial \dot{\mathbf{d}}} \right) \right] - \rho \mathbf{b} + \text{div} \left[\mathbf{p} - \text{div} \left(\frac{\partial \phi}{\partial \text{grad } \dot{\mathbf{d}}} \right) \right] = 0,$$

where the additional dependence is described by the Rayleigh-like dissipation function $\phi = \phi(\dot{\mathbf{d}}, \text{grad } \dot{\mathbf{d}})$ which fulfills, from the definition, the perpetuum mobile principles.

In a recent explanation of the problem of the second-order derivative of velocity, FRIED and GURTIN [72] assuming only the gradient of $\dot{\mathbf{d}}$: $\phi = \phi(\text{grad } \dot{\mathbf{d}})$, have defined the hyper-viscous stress triad $\mathbf{G} = G_{ijk} \mathbf{e}_i \otimes \mathbf{e}_j \otimes \mathbf{e}_k$:

$$(5.3) \quad \mathbf{G} = \frac{\partial \phi}{\partial \text{grad } \dot{\mathbf{d}}} \\ = \eta_1 \text{grad}(\text{grad } \dot{\mathbf{v}}) + \eta_2 [\text{grad}^T(\text{grad}^T \dot{\mathbf{v}}) + \text{grad}^T(\text{grad } \dot{\mathbf{v}}) - \mathbf{I} \otimes \text{lap } \dot{\mathbf{v}}]$$

with two additional internal viscous friction coefficients η_1, η_2 . Thus, they have obtained the following momentum balance in the bulk:

$$(5.4) \quad \rho(\dot{\mathbf{v}} - \mathbf{b}) + \text{div}(\mathbf{p} - \text{div } \mathbf{G}) = 0$$

and not one, but two boundary conditions coming from making the Green transformation twice [68]:

$$(5.5) \quad \begin{aligned} \mathbf{p}_n &= \mathbf{p}\mathbf{n} - (\operatorname{div} \mathbf{G})\mathbf{n} - \operatorname{div}_s(\mathbf{G}\mathbf{n}) - \mathbf{I}_b(\mathbf{G}\mathbf{n})\mathbf{n}, \\ \mathbf{m}_n &= (\mathbf{G}\mathbf{n})\mathbf{n}. \end{aligned}$$

These are nothing less than an extension of the classical Cauchy definition of the traction force $\mathbf{p}_n = \mathbf{p}\mathbf{n}$. The first traction force is working on a field of velocity [like the classical Umov flux of mechanical energy] and the second fraction vector \mathbf{m}_n , new in the context of a viscous fluid, is to work on the normal derivative of velocity $\partial\mathbf{v}/\partial\mathbf{n}$. Therefore, FRIED and GURTIN postulate the following slip and adherence condition [47]:

$$(5.6) \quad \nu(\mathbf{v}_A - \mathbf{v}_{\text{wall}}) = \mathbf{p}_n \quad (\text{generalized slip condition}),$$

$$(5.7) \quad \nu_a \left(\frac{\partial\mathbf{v}_A}{\partial\mathbf{n}} - \frac{\partial\mathbf{v}_{\text{wall}}}{\partial\mathbf{n}} \right) = \mathbf{m}_n \quad (\text{generalized adherence condition}).$$

Here, $\nu = \mu/l_s$; $\nu_a = \eta_1/l_a$ are the external friction and external adherence friction coefficients, respectively. l_s and l_a represent the slip length and the adherence length. This model of boundary layer is fully consistent with Fried and Gurtin's bulk model of the second-order fluid, and cover Deissler's Eq. (5.1).

6. Poiseuille, Knudsen and Reynolds components of the filtration velocity

A peculiar difficulty in the modeling of flow in porous media often arises if we are forced to apply the so-called "non-Darcy equation". Or if we try to develop some extension of the Darcy equation such as the Brinkmann–Darcy–Forchheimer equation [73]. Moreover, trying to develop a model from which one can describe the Klinkenberg effect, i.e. different permeability of a porous media for different gases, one should take into account the velocity slip and the temperature jump [74–76].

But also the state of phenomenological level of modeling is far from clear due to the lack of the accumulation of knowledge from several separate fields of application. In our opinion, there is no exchange of information and ideas between various fields involved with flow in porous media, therefore the Darcy equation is always given *ex cathedra*.

Treating a nano-pipe as equivalent to a single porous domain and looking for common effects of the bulk and surface motion, one can consider the following momentum flux integral in any cross section of a porous media oriented by the

tangential component of unit vector \mathbf{n}_{tan} :

$$(6.1) \quad \iint_{\text{bulk section}} (\rho \mathbf{v} \otimes \mathbf{v} + \mathbf{p}) \mathbf{n}_{\text{tan}} dA + \oint_{\mathcal{C}} (\rho_s \mathbf{v}_s \otimes \mathbf{v}_s + \mathbf{p}_s + \mathbf{n}_{\text{nor}} \mathbf{p} + \mathbf{f}_{\partial V}) \mathbf{n}_{\text{tan}} d\mathcal{C} = 0.$$

In the above $\rho \mathbf{v}$ and $\rho_s \mathbf{v}_s$ are the bulk and the surface momentum density vectors, ρ and ρ_s are the gas density in the bulk and on the boundary. Next, $\mathbf{p} = p_{ij} \mathbf{e}_i \otimes \mathbf{e}_j = \mathbf{p}^T$ and $\mathbf{p}_s = \mathbf{p}_s^T$ are the bulk and the surface flux of momentum.

Let us define the total momentum influx to be:

$$(6.2) \quad \mathcal{M} = \iint_{\text{bulk section}} \rho \mathbf{v} u_{\text{tan}} dA + \oint_{\mathcal{C}} \rho_s \mathbf{v}_s u_{s \text{ tan}} d\mathcal{C}.$$

This consists of contributions from the bulk velocity and from the slip velocity. Hence, $\iint_{\text{bulk section}} \rho \mathbf{v} u_{\text{tan}} dA$ is a contribution from the bulk velocity and $\oint_{\mathcal{C}} \rho_s \mathbf{v}_s u_{s \text{ tan}} d\mathcal{C}$ is a contribution from the surface (slip) velocity. Using some principals from a technique of homogenization, we assume the existence of a resultant velocity, say \mathbf{v}_r , which is parallel to the vector of total momentum:

$$(6.3) \quad \mathcal{M} = \dot{m} \mathbf{v}_r.$$

It is located somewhere in the geometrical center of the velocity profile. In many cases, independently of the shape of the cross section, the bulk profile of velocity is nearly flat and ending with value of $u_{s \text{ tan}}$ – the magnitude of slip velocity. In the above, in accordance with traditional Reynolds notation, denotes the resultant mass flow rate. Remembering that the boundary force $\mathbf{f}_{\partial V} = \mathbf{f}_r + \mathbf{f}_m = \nu(\mathbf{v} - \mathbf{v}_{\text{wall}}) - [c_{m\theta} \text{grad}_s \theta_s + \dots]$ is a composition of friction forces and mobility forces, we can reorganize the integral (6.1), expressing explicitly the thermal mobility part $c_{m\theta} \text{grad}_s \theta_s$ and the slip friction part $\nu \mathbf{v}_s \mathbf{I}_s$:

$$(6.4) \quad \dot{m} \mathbf{v}_r = \iint_{\text{Poiseuille}} [p \mathbf{I} + 2\mu \mathbf{d}] \mathbf{n} dA + \oint_{\text{Darcy}} \nu \mathbf{v}_s \mathbf{I}_s d\mathcal{C} - \oint_{\text{Reynolds}} c_{m\theta} \text{grad}_s(\theta_s) d\mathcal{C} + \dots$$

Since the cross section of porous media is quite arbitrary, that a known procedure of homogenization can be applied, and Eq. (6.4) leads to 3D resultant

equations [74]:

$$(6.5) \quad \text{Poiseuille} = -\dot{m} \frac{P}{\mu} \mathbf{B} \frac{\text{grad } P}{P},$$

$$(6.6) \quad \text{Knudsen} = -\dot{m} \mathbf{D}_K \frac{\text{grad } P}{P},$$

$$(6.7) \quad \text{Reynolds} = +\dot{m} \mathbf{D} \frac{\text{grad } T}{T}.$$

Here, the surface pressure p_s does not appear, nor does the surface temperature θ_s , since after homogenization their role takes the capillarity pressure P and the capillarity temperature T . Also, the two-dimensional surface gradient, due to homogenization, becomes the three-dimensional gradient $\text{grad}(\cdot)$. Finally, the Poiseuille–Knudsen–Reynolds equations possess the form [74]:

$$(6.8) \quad \mathbf{v}_r = - \left(\frac{P}{\mu} \mathbf{B} + \mathbf{D}_K \right) \frac{\text{grad } P}{P} + \mathbf{D} \frac{\text{grad } T}{T},$$

where \mathbf{v}_r is the resultant filtration velocity, μ is a gas viscosity, \mathbf{B} is the permeability tensor, \mathbf{D}_K is the Knudsen accommodation diffusion tensor and \mathbf{D} is the thermal transpiration coefficient tensor. The sign of \mathbf{D} is indeed negative, which means that gas has tendency to flow toward the hotter side of a porous body.

It is useful here to recall that rarefied gas flow through a porous media in non-isothermal conditions is mathematically described by the so-called ‘‘Dusty-Gas-Model’’ (DGM) [77], which is an appropriate approximation of the kinetic theory of gases within the slip-flow regime. In contrast to the DGM model, we have shown that, the continuous model (6.8) is also obeying the slip-flow regime. The model (6.8) insists on a combination of an effective viscous Poiseuille bulk flow, a Knudsen surface slip-driven flow and a Reynolds surface thermally-driven flow. This phenomenological model is based on the previously averaged equations for the bulk flow resistance and the surface mobility forces.

7. Conclusions

Despite the fact that investigation of slip-flow and thermal transpiration started long ago, many questions remain unresolved. This is connected with a special feature of thermal transpiration, which is very sensitive to the kind of solid material and the kind of rarefied gas. Thermal mobility force $\mathbf{f}_m = -c_{m\theta} \text{grad}_s \theta$ proposed by Reynolds and Maxwell [on the ground of kinetic theory] is, in general, sensitive to properties of both gas and solid surfaces and additionally depends on two thermal momentum accommodation coefficients f_3 , f_4 proposed by REYNOLDS [5]. However, thermal mobility force can also be de-

veloped within the framework of continuum modeling with consistent closure to the $c_{m\theta}$. The coefficient $c_{m\theta}$ should be based on complete experimental data.

The rising interest in the Knudsen pump and the accommodation pump is connected with the problem of temperature dependence of both the friction ν and thermal mobility $c_{m\theta}$ coefficients. Quite new devices based on an increased understanding of the influence of slip conditions and thermal mobility are under development for the power industry. These devices mainly include: 1) a wet combustion chamber using oxy-combustion and water cooling by thermal transpiration; 2) a spray-ejector condenser (using bulk condensation on the surface of steam-gas water droplets); 3) gas turbine blades. The walls of combustion chambers and the bodies of turbine blades are created as porous structures. Using such porous structures or structures with microchannels, bringing the cooling fluid closer to the surface ensures that a much stronger uniformity of cooling and thermal gradients are obtained [78]. The research on combustion chambers with thermal transpiration or microholes cooling effectiveness can be described more accurately taking into account the surface friction force and surface mobility force. In this connection it is of interest to consider effective boundary conditions for an extremely irregular surface with nano-patterns [79, 80]. Then the friction force becomes non-parallel to a vector of slip velocity and the thermal mobility force is not parallel to a surface gradient of temperature. This kind of anisotropy requires a deeper experimental set-up [81].

The model of thermal mobility force, revalorized here after Maxwell and numerically proven in [61], can be, in our opinion, also extended to the so-called second-order continuum model but only if we simultaneously redefine the stress tensor, adding the hyper-stress (5.3), and supplement a boundary condition in the form of Eq. (5.5).

Finally, the result of joint action of the both surface Navier slip and Maxwell thermal mobility may be predicted by measuring gas mass flow rates in porous materials. If the pores are larger than 2–5 times the free length of the rarefied gas, then an additional bulk contribution of viscous flow (Poiseuille's type) is visible and the mass flow rate is the summary effect of one bulk and two surface contributions. Thus, as we have shown in Sec. 6, the resultant flow velocity of filtration governed by the Poiseuille–Knudsen–Reynolds Eq. (6.8). It is an analogy of Maxwell's equation for a long cylindrical pore. Equation (6.8) may help at least to decrease the number of experimental attempts to find the proper composition of an experimental set up [74].

References

1. C.P. CELATA, M. CUMO, S.J. MCPHALL, L. TEFAGBIR, G. ZUMMO, *Experimental study on compressible flow in microtubes*, International Journal of Heat and Fluid Flow, **28**, 28–36, 2007.

2. S. COLIN, *Rarefaction and compressibility effects on steady and transient gas flows in microchannels*, *Microfluidics and Nanofluidics*, **1**, 3, 268–279, 2005.
3. G.E. KARNIADAKIS, A. BESKOK, N. ALURU, *Microflows and Nanoflows: Fundamentals and Simulation*, Springer, New York, 2005.
4. G.L. MORINI, Y. YANG, H. CHALABI, M. LORENZINI, *A critical review of the measurement techniques for the analysis of gas microflow through microchannels*, *Experimental Thermal and Fluid Science*, **35**, 849–893, 2011.
5. O. REYNOLDS, *On certain dimensional properties of matter in the gaseous state Part I. Experimental researches on thermal transpiration of gases through porous plates and on the laws of transpiration and impulsion, including an experimental proof that gas is not a continuous plenum. Part II. On an extension of the dynamical theory of gas, which includes the stresses, tangential and normal, caused by a varying condition of gas, and affords an explanation of the phenomena of transpiration and impulsion*, *Philosophical Transactions of the Royal Society of London*, **170**, 727–845, 1879.
6. O. REYNOLDS, *On the equation of motion and the boundary conditions for viscous fluid* (1883), *Scientific Papers on Mechanics and Physical Subjects*, Vol. 2, **46**, 132–137, Cambridge University Press, Cambridge, 1901.
7. J.C. MAXWELL, *On stresses in rarified gases arising from inequalities of temperature*, *Philosophical Transactions of the Royal Society of London*, **170**, 231–256, 1879.
8. C.M. HO, Y.C. TAI, *Micro-Electro-Mechanical-Systems (MEMS) and fluid flow*, *Annual Review of Fluid Mechanics*, **30**, 579–612, 1998.
9. M. GAD-EL-HAK, *The fluid mechanics of microdevices*, *Journal of Fluids Engineering*, **12**, 1, 5–33, 1999.
10. M. GAD-EL-HAK, *Handbook of MEMS*, CRC Press, New York, 2001.
11. H. GARDENIERS, A. VAN DEN BERG, *Micro- and nanofluidic devices for environmental and biomedical applications*, *International Journal of Environmental Analytical Chemistry*, **84**, 809–819, 2004.
12. M. HOSSEINI, M. SADEGHI-GOUGHARI, S.A. ATASHIPOUR, M. EFTEKHARI, *Vibration analysis of single-walled carbon nanotubes conveying nanoflow embedded in a viscoelastic medium using modified nonlocal beam model*, *Archives of Mechanics*, **66**, 4, 217–244, 2014.
13. J. MAURER, P. TABELING, P. JOSEPH, H. WILLAIME, *Second order slip laws in microchannels for helium and nitrogen*, *Physics of Fluids*, **15**, 2613–2621, 2003.
14. P.A. THOMSON, S.M. TROJAN, *A general boundary condition for liquid flow at solid surface*, *Nature*, **389**, 360–362, 1997.
15. A. BESKOK, G.E. KARNIADAKIS, *A model for flows in channels, pipes, and ducts at micro and nano scales*, *Microscale Thermophysical Engineering*, **3**, 43–77, 1999.
16. P. ZIÓLKOWSKI, J. BADUR, *Navier number and transition to turbulence*, *Journal of Physics: Conference Series*, **530**, 012035, 2014, doi:10.1088/1742-6596/530/1/012035.
17. J. BADUR, P.J. ZIÓLKOWSKI, P. ZIÓLKOWSKI, *On the angular velocity slip in nano flows*, *Microfluidics and Nanofluidics*, **19**, 191–198, 2015.
18. R.G. DEISSLER, *An analysis of second-order slip flow and temperature jump boundary conditions for rarefied gases*, *International Journal of Heat and Mass Transfer*, **7**, 681–694, 1964.

19. S. COLIN, P. LALONDE, R. CAEN, *Validation of a second-order slip flow model in rectangular microchannels*, *Heat Transfer Engineering*, **25**, 23–30, 2004.
20. M.N. KOGAN, *Rarefied Gas Dynamics*, Plenum Press, New York, 1969.
21. E.B. ARKILIC, M.A. SCHMIDT, K.S. BREUER, *Gaseous slip flow in long microchannels*, *Journal of Microelectromechanical Systems*, **6**, 167–178, 1997.
22. G.L. MORINI, M. LORENZI, M. SPIGA, *A criterion for experimental validation of slip-flow models for incompressible rarefied gases through microchannels*, *Microfluidics and Nanofluidics*, **1**, 190–196, 2005.
23. J. PITAKARNNOP, S. VAROUTIS, D. VALOUGERGIS, S. GEOFFROY, L. BALDAS, S. COLIN, *A novel experimental setup for gas microflows*, *Microfluidics and Nanofluidics*, **8**, 57–72, 2010.
24. I. NEWTON, *Philosophiæ Naturalis Principia Mathematica*, London, 1726, 3rd edition, H. Pemberton, A. Motte [eds.], *Sir Isaac Newton's Mathematical Principles of Natural Philosophy and His System of the World*, London, 1729, [revised] University of California Press, California, 1962.
25. W. PIETRASZKIEWICZ, *Refined resultant thermomechanics of shells*, *International Journal of Engineering Science*, **49**, 1112–1124, 2011.
26. C. TRUESDELL, R. TOUPIN, *The Classical Field Theories*, *Principles of Classical Mechanics and Field Theory*, Series: Encyclopedia of Physics (Prinzipien der Klassischen Mechanik und Feldtheorie, Handbuch der Physik), S. Flügge [Ed.], vVol. 2/3/1, 226–858, Springer, Berlin, 1960.
27. O. DARRIGOL, *Between hydrodynamics and elasticity theory: the first five births of the Navier–Stokes equation*, *Archive for History of Exact Sciences*, **56**, 95–150, 2002.
28. S. POISSON, *Mémoire sur les Equations générales de l'équilibre et du mouvement des Corps solides, élastiques et fluids*, *Essay on the general equation of equilibrium motion of a solid body in elastic fluids*, *Journal de l'Ecole Polytechnique*, **13**, 1–174, 1829 [in French].
29. L. NATANSON, *On the laws of viscosity*, *Philosophical Magazine*, **2**, 342–356, 1901.
30. L. PRANDTL, *Über Flüssigkeitsbewegung bei sehr kleiner Reibung*, *On the motion of fluids of very small viscosity*, [in:] *Verhandlungen des dritten internationalen Mathematiker-Kongresses in Heidelberg*, 484–491, 1904 [in German].
31. J. BADUR, *Rozwój pojęcia energii*, *Development of Energy Concept*, IMP PAN Publishers, Gdańsk, 2009 [in Polish].
32. M. KAR CZ, J. BADUR, *Numeryczna implementacja modelu racjonalnej turbulencji*, *Numerical implementation of rational turbulence model*, *Scientific Bulletin Institute Fluid Flow Machinery PAS*, **531**, 1490/2003, 1–34, 2003 [in Polish].
33. R.W. BARBER, D.R. EMERSON, *Challenges in modeling gas-phase flow in microchannels: from slip to transition*, *Heat Transfer Engineering*, **27**, 3–12, 2006.
34. J. BADUR, M. KAR CZ, M. LEMAŃSKI, L. NASTALEK, *Foundations of the Navier-Stokes boundary conditions in fluid mechanics*, *Transactions of the Institute of Fluid-Flow Machinery*, **123**, 3–55, 2011.
35. N. DONGARI, A. SHARMA, P. DURST, *Pressure-driven diffusive gas flows in microchannels: from the Knudsen to the continuum regimes*, *Microfluidics and Nanofluidics*, **6**, 679–692, 2009.

36. M. KAR CZ, J. BADUR, *An alternative two-equation turbulent heat diffusivity closure*, International Journal of Heat and Mass Transfer, **48**, 2013–2022, 2005.
37. V.K. MICHALIS, A.N. KALARAKIS, E.D. SKOURAS, V.N. BURGANOS, *Rarefaction effects on gas viscosity in the Knudsen transition regime*, Microfluidics and Nanofluidics, **9**, 847–853, 2010.
38. T.G. MYERS, *Why are slip lengths so large in carbon nanotubes?*, Microfluidics and Nanofluidics, **10**, 1141–1145, 2011.
39. J. D’ALEMBERT, *Essai d’une Nouvelle Théorie de la Résistance des Fluids, Essay of a New Theory of Resistance of Fluids*, David, Paris, 1752 [in French].
40. C.A. COULOMB, *Expériences destinées à déterminer la cohérence des fluides et les lois de leur résistance dans les mouvement très lents, Experiments to determine the coherence of fluids and laws of their resistance in very slow movements*, Mémoires de l’Institut National des Sciences et Arts – Mémoires de Mathématiques et de Physique, **3**, 246–305, 1801 [in French].
41. K. KAMRIN, H.A. STONE, *The symmetry of mobility laws for viscous flow along arbitrarily patterned surfaces*, Physics of Fluids, **23**, 031701, 2011.
42. C. TRUESDELL, *Rational Fluid Mechanics*, Orell Füssil, Zürich, pp. 1687–1765, 1954.
43. M. FEIDT, *Finite Physical Dimensions Optimal Thermodynamics. 1 Fundamentals*, ISTE Press /Elsevier, London, 2017.
44. P. DUHEM, *Reserches sur l’hydrodynamique, Research on hydrodynamics*, Annales de la Faculté des Sciences de Toulouse, **5**, 4, 353–404, 1903 [in French].
45. C.L.M.H. NAVIER, *Mémoire sur les lois du mouvement des fluides, Memory on the laws of fluid motion*, Mémoires l’Académie Royale des Sciences de l’Institut de France, **6**, 389–440, 1827 [in French].
46. D.L. MORRIS, A. HANNON, A.L. GARCIA, *Slip length in a dilute gas*, Physical Review A, **46**, 5279–5282, 1992.
47. J. BADUR, M. KAR CZ, M. LEMAŃSKI, *On the mass and momentum transport in the Navier–Stokes slip layer*, Microfluidics and Nanofluidics, **11**, 439–449, 2011.
48. T.E. STANTON, J.R. PANNELL, *Similarity of motion in relation to the surface friction of fluids*, Philosophical Transactions of the Royal Society of London, **214**, 199–221, 1914.
49. S. COLIN, *Single-phase gas flow in microchannels*, [in:] S. Kandlikar *et al.*, *Heat Transfer and Fluid Flow in Minichannels and Microchannels*, Elsevier, Oxford, 9–86, 2006.
50. J. BADUR, M. KAR CZ, M. LEMAŃSKI, L. NASTALEK, *Enhancement transport phenomena in the Navier–Stokes shell-like slip layer*, CMES: Computer Modeling in Engineering & Sciences, **73**, 299–310, 2011. doi:10.3970/cmcs.2011.073.299.
51. J. BADUR, P. ZIÓLKOWSKI, W. ZAKRZEWSKI, D. SŁAWIŃSKI, M. BANASZKIEWICZ, O. KACZMARCZYK, S. KORNET, P.J. ZIÓLKOWSKI, *On the surface vis impressa caused by a fluid-solid contact*, [in:] Shell Structures: Theory and Applications, W. Pietraszkiewicz & J. Górski [eds.], **3**, 53–56, 2014.
52. W. CROOKES, *On repulsion resulting from radiation. Parts III & IV*, Philosophical Transactions of the Royal Society of London, **166**, 325–376, 1876.
53. J. TYNDALL, *On Dust and Disease*, W. Clowes and Sons, London, 1870.

54. D.A. EDWARDS, H. BRENNER, *Interfacial Transport Processes and Rheology*, Butterworth-Heinemann, Boston, 1991.
55. H. HELMHOLTZ, G. VON PIOTROWSKI, *Über Reibung von opfbarer Flüssigkeiten, Abrasion of opaque liquids* [in]: Wissenschaftliche Abhandlungen *Flüssigkeiten*, Scientific Papers, H. Helmholtz, J. A. Barth [eds.], Leipzig, 172–222, 1882 [in German].
56. A. KNUDT, E. WARBURG, *Ueber Reibung und Wärmeleitung verdünnter Gase, On friction and heat conduction of dilute gases*, *Annalen der Physik*, **231**, 7, 337–365, 1875; **232**, 10, 177–211, 1875 [in German].
57. J. BADUR, B.H. SUN, *Some remarks on the structure of evolution equations*, *Applied Mathematics and Mechanics*, **16**, 747–757, 1995.
58. S.S. HSIEH, H.H. TSAI, C.Y. LIN, C.F. HUANG, C.M. CHIEN, *Gas flow in a long microchannel*, *International Journal of Heat and Mass Transfer*, **47**, 3877–3887, 2004.
59. J.T.C. LIU, M.E. FULLER, K. L. WU, A. CZULAK, A.G. KITHES, C.J. FELTEN, *Nanofluid flow and heat transfer in boundary layers at small nanoparticle volume fraction: zero nanoparticle flux at solid wall*, *Archives of Mechanics*, **69**, 75–100, 2017.
60. J.R. BIELENBERG, H. BRENNER, *A continuum theory of thermal transpiration*, *Journal of Fluid Mechanics*, **546**, 1–23, 2006.
61. P. ZIÓŁKOWSKI, J. BADUR, *A theoretical, numerical and experimental verification of the Reynolds thermal transpiration law*, *International Journal of Numerical Methods for Heat and Fluid Flow*, **28**, 1, 64–80, 2018, <https://doi.org/10.1108/HFF-10-2016-0412>.
62. D.A. LOCKERBY, A. PATRONIS, M.K. BORG, J.M. REESE, *Asynchronous coupling of hybrid models for efficient simulation of multiscale systems*, *Journal of Computational Physics*, **284**, 261–272, 2015.
63. A. KUCABA-PIĘTAL, *Microchannels flow modelling with the micropolar fluid theory*, *Bulletin of the Polish Academy of Sciences: Technical Sciences*, **52**, 209–214, 2004.
64. T.A. KOWALEWSKI, P. NAKIELSKI, F. PIERINI, K. ZEMBRZYCKI S. PAWŁOWSKA, *Micro and nano fluid mechanics*, [in]: *Advances in Mechanics: Theoretical, Computational and Interdisciplinary Issues*, M. Kleiber *et al.* [eds.], 27–34, 2016.
65. A. KUCABA-PIĘTAL, Z. WALENTA, Z. PERADZYŃSKI, *Molecular dynamics computer simulation of water flows in nanochannels*, *Bulletin of the Polish Academy of Sciences: Technical Sciences*, **57**, 55–61, 2009.
66. F.C. GOODRICH, *The theory of capillarity excess viscosities*, *Proceedings of the Royal Society A*, **374**, 341–370, 1981.
67. T.S. STORVICK, H.S. PARK, S.K. LOYALKA, *Thermal transpiration: a comparison of experiment and theory*, *Journal of Vacuum Science and Technology*, **15**, 1844–1852, 1978.
68. M. ROJAS-CÁRDENAS, I. GRAUR, P. PERRIER, J.G. MEOLANS, *Thermal transpiration flow: A circular cross-section microtube submitted to a temperature gradient*, *Physics of Fluids*, **25**, 031702, 2011.
69. J.M. REESE, Y. ZHENG, D.A. LOCKERBY, *Computing the near-wall region in gas micro- and nanofluidics: critical Knudsen layer phenomena*, *Journal of Computational and Theoretical Nanoscience*, **4**, 807–813, 2007.
70. T. EWART, P. PERRIER, P.I. GRAUR, J.G. MEOLANS, *Tangential momentum accommodation in microtubes*, *Microfluidics and Nanofluidics*, **3**, 689–695, 2007.

71. E.H. KENNARD, *Kinetic Theory of Gases: with an Introduction to Statistical Mechanics*, McGraw-Hill Book Company, New York, 1938.
72. E. FRIED, M.E. GURTIN, *Tractions, balances and boundary conditions for nonsimple materials with application to liquid flow at small-length scales*, *Archive for Rational Mechanics and Analysis*, **182**, 513–554, 2005.
73. K. HOOMAN, *Heat and fluid flow in a rectangular microchannel filled with a porous medium*, *International Journal of Heat and Mass Transfer*, **51**, 5804–5810, 2008.
74. G.L. VIGNOLES, P. CHARRIER, C. PREUX, B. DUBROCA, *Rarefied pure gas transport in non-isothermal porous media: effective transport properties from homogenization of the kinetic equation*, *Transport in Porous Media*, **73**, 211–232, 2008.
75. M.T. MATTHEWS, J.M. HILL, *On thee simple experiments to determine slip lengths*, *Microfluidics and Nanofluidics*, **6**, 611–619, 2009.
76. P. DE GENNES, F. BROCHARD-WYART, D. QUERE, *Capillarity and Wetting Phenomena*, Springer, New York, 2004.
77. K. VAFAI, C.L. TIEN, *Boundary and inertial effects on flow and heat transfer in porous media*, *International Journal of Heat and Mass Transfer*, **24**, 195–203, 1981.
78. T. OCHRYMIUK, *Numerical analysis of microholes film/effusion cooling effectiveness*, *Journal of Thermal Science*, **26**, 5, 459–464, 2017.
79. R.N. MOGHADDAM, M. JAMIOLAHMADY, *Slip flow in porous media*, *Fuel*, **173**, 298–310, 2016.
80. P. KRAKOWSKA, P. MADEJSKI, J. JARZYNA, *Permeability estimation using CFD modeling in tight Carboniferous sandstone*, 76th EAGE Conference & Exhibition 2014 Amsterdam RAI, doi: 10.3997/2214-4609.20141607, 2014.
81. C.B. SOBHAN, G.P. PETERSON, *Microscale and Nanoscale Heat Transfer Fundamentals and Engineering Applications*, CRC Press, Taylor & Francis Group, Boca Raton, 2008.

Received September 30, 2017; revised version March 27, 2018.
